Bachelor Research Project Physics

Simulating Cold Three-Body Recombination of Antihydrogen

Author:
Joël P. Zwart
S3146022

First Examiner:
Dr. S.A. Jones
Second Examiner:
Dr. J. Even

Abstract

Three-body recombination is believed to be the primary pathway for antihydrogen formation in "cold" (<30 K) conditions, like at the ALPHA collaboration. A method for the classical simulation of three-body recombination resulting in antihydrogen will be outlined. Considerations of the simulation methodology will also be examined. This method is utilised to simulate many antihydrogen formation events resulting from three-body interactions. The binding energies of the resulting antihydrogen are found to be in the order of the thermal energy of the formation environment, indicating a low survival chance immediately after formation. The model offers a starting point for further study of the efficiency of antihydrogen generation and measurement.

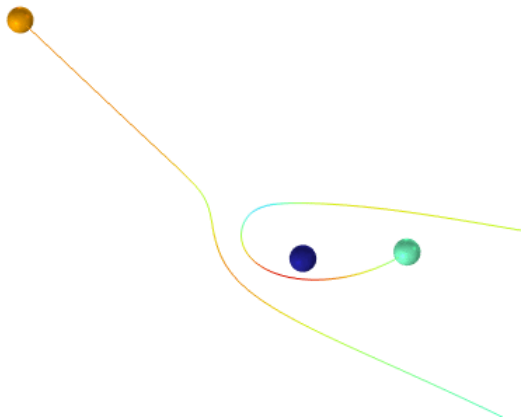

Faculty of Science and Engineering
University of Groningen
Groningen, the Netherlands
July 2023

Contents

1 Introduction

Antimatter has been intensely studied ever since its first observation in 1932 by Carl Anderson, four years after being predicted by Paul Dirac [1, 2]. Despite knowledge about the particles existing for nearly 100 years important aspects of the exotic matter are still unknown. For example, the gravitational mass of an antiparticle has never been directly measured. It is also unknown why so little antimatter is found naturally in our universe. The CPT-theorem states that whenever you apply a CPT transformation to a particle, the physical laws that govern it should be indistinguishable from the non-transformed particle. This CPT transformation is a simultaneous application of charge conjugation, time reversal and parity transformations. Antimatter is CPT transformed matter, so as a result it should have the same properties as matter, with the exception of those directly changed by the CPT transformation. The established theory also predicts that antimatter and matter should be formed in the same quantities. However, it seems this symmetry is not kept when looking at the actual composition of matter in the observable universe. This disparity between the observation and the theory remains unanswered.

When an inconsistency between theory and observation arises in physics it is usually because of a mechanism that has not been incorporated into theory. By understanding and resolving the inconsistency new physics can potentially be discovered. To truly understand the properties of antimatter a number of experiments are investigating various aspects that could lead to new insights. One of the areas of interest is the study of antihydrogen, containing an antiproton and a positron. CPT predicts that the energy levels of antihydrogen should be precisely the same as hydrogen, a well understood and measured atom. As a result comparisons could be made between hydrogen and antihydrogen.

A couple experiments focus on antihydrogen production, containment and measurement. The one that has been running the longest is ALPHA at CERN, having successfully produced and trapped many antihydrogen atoms. Spectroscopy has been preformed on the trapped antihydrogen and the 1s-2s emission line was measured to be equal to that of hydrogen up to a level of 2×10^{-12} [3]. Despite these successes it remains difficult to produce large quantities trappable antihydrogen. In order to produce it, a large number of antiprotons and positrons are combined in a Penning trap. The antihydrogen needs to not only be produced but also trapped. This is done by using a neutral atom trap. For the atoms to be trappable they need to be cold (< 0.5 K). This greatly limits the number of antihydrogen atoms that can actually be trapped as only a small fraction is below this temperature.

The most prevalent path to antihydrogen is believed to be the three-body recombination process. Here three bodies, two positrons and one antiproton, interact in such a way that in the end a single antihydrogen atom remains. Since it is not possible to fully solve this interaction analytically, other approaches will have to be employed By doing simulations of antihydrogen formation better insights could be gained into this recombination. In addition, various parameters could be investigated. By doing this investigation optimal parameters might be found that could potentially have been missed due to the considerations of the setup. Due to the nature of the experiment insight cannot always be gained by measurements; some processes are not measurable and need to therefore be simulated. Some areas of interest are the binding energies of the positrons in the antihydrogen atom, as previously investigated by Robichaux and Jonsell et al. [4, 5]. By approximating the system computationally the goal of this investigation is to accurately simulate the three-body recombination process leading to antihydrogen, and study the properties of the newly formed anti-atoms.

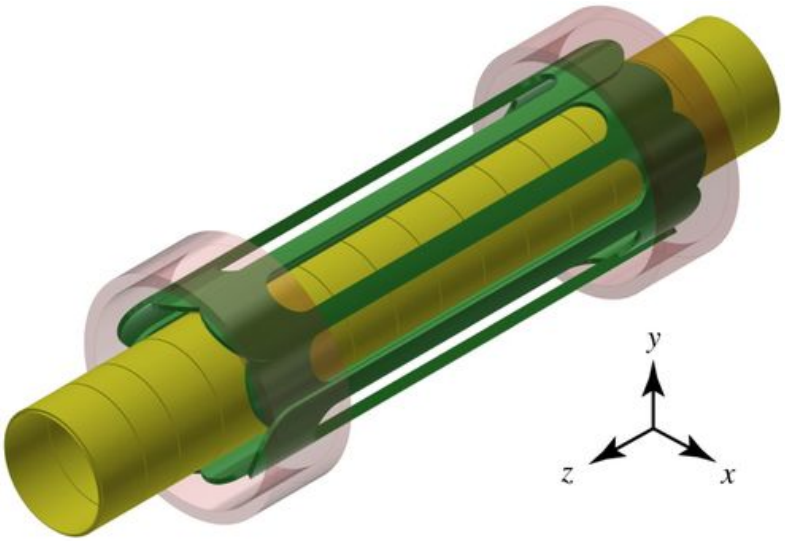

Figure 1: The mixing trap at the ALPHA experiment. The electrodes of the Penning trap are shown in yellow, the neutral atom trap in green and red. The external solenoid magnet is not pictured. Its field is directed in the z-axis. Figure from Bertsche [8]

.

2 The ALPHA Experiment

To understand what will need to be simulated, it is useful to walk trough the experiment whose conditions will need to be simulated. At APLHA, antihydrogen is produced by combining positrons and antiprotons in a trap. The positrons are first produced, cooled and subsequently guided into the main mixing trap by shifting the potential of electrodes leading to the mixing trap. The antiprotons are carried into the trap in similar fashion, but also have to be slowed from their initial MeV range velocities. The positrons are numerous in availability while the antiprotons are harder to come by, mainly due to the need to slow them down which leads to $\sim$ 97% being lost. While the number of captured positrons is typically 100 million, antiprotons are only captured at roughly 100,000 at a time. After being caught, the antiprotons still need to be cooled further, this happens by sympathetically cooling them via interactions with electrons, and by evaporative cooling after the electrons have been removed (see e.g. Amole et al. [6] for more). The latter method causing additional antiprotons to be lost. After the cooling steps both the antiprotons and the positrons are at a temperature of about 20 K, with the positrons often being colder then the antiprotons. The temperature of the positrons seems play a more important role for antihydrogen formation than that of the antiprotons[7].

The mixing section of the setup consists out of a Penning-Malmberg trap to contain the charged particles, and a neutral atom trap, a Ioffe trap, to capture the antihydrogen once it forms and survives long enough to reach the ground state. The trap excluding the external solenoid used to generate the axial magnetic field is shown in figure 1. The Ioffe trap consists out of a octupolar superconductor and two mirror coils. These elements form a magnetic minimum, trapping any ground state antihydrogen in a low field seeking state. The low field seeking state causes the antihydrogen to interact with the magnetic field in such a way as to produce a force in the negative gradient direction of the magnetic field. In case of a magnetic minimum this would be a restoring force towards the center of the trap [9]. The entire mixing section is kept at a low temperature ($\sim$4 K) in order to provide cooling for the superconductors of the Ioffe trap. As mentioned before the neutral atom trap is only 0.8 T deep, which corresponds to an energy required by an antihydrogen particle to escape such a trap of 0.54 K (where multiplication by k_B is implicit to obtain energy).

The Penning-Malmberg trap is the component responsible for mixing the two particle species and combining them into the neutral antihydrogen atom. As mentioned this is achieved by manip-

ulating the potentials of the electrodes on the Penning trap until the two particle clouds meet. The mechanism of how a Penning trap contains neutral particles is treated in more detail in section 3.1. After production the antihydrogen will be trapped by the neutral atom trap. Even with the colder temperatures involved, the amount of antihydrogen that can be captured is rather low, only a small fraction of the antihydrogen is cold enough to meet the 0.5 K requirement. Not only will the formed antihydrogen often be too "hot" to be capturable, it could also be in a non low field seeking state, causing it to escape confinement As a result of these factors the amount of antihydrogen that is usable for measurement is very low. This means that in order to obtain enough antihydrogen, multiple mixing cycles are necessary, the products of each run being stored in the neutral atom trap during the subsequent cycles. This process is also referred to as stacking. After 5 cycles the number of antihydrogen atoms captured total 54 ± 6 and increase by 10.5 ± 0.6 per cycle [10]. After capturing measurements can be performed (for example [3, 11]).

3 Theory

3.1 Particle Dynamics in a Penning Trap

The motions of charged particles as contained in a Penning trap are generally well understood from an analytical perspective. A Penning trap utilizes the combination of a magnetic and electric field to contain charged particles (trapping them). It does this by creating an electric potential that can be expanded as a standard harmonic potential around zero (the center of the trap). By applying this potential the resulting electric field will contain the particles axially. It will, however, accelerate the charged particles in the radial direction, causing them to leave the trap. This is where the magnetic field becomes relevant. By applying a strong magnetic field in the axial direction, perpendicular to the acceleration of the particles due to the electric field, these particles will experience a force in the $\mathbf{E} \times \mathbf{B}$ direction. If the magnetic field is strong enough in comparison to the electric field the particle will be completely deflected back into the trap. The combination of the axial confinement by the electric and the radial confinement by the magnetic field, cause the particle to be trapped.

When solving the equations of motions a number of modes of motion can be identified. In general the particle will oscillate in the axial direction. Due to the fact that the axial potential is a harmonic potential and the influence of the axial magnetic field is zero, the motion in the z axis will be a simple harmonic motion (z being the axial direction). The frequency of oscillation being

$$\omega_z^2 = \frac{q\mathrm{U}}{md^2}. \tag{1}$$

Where q and m are are the charge and mass of the particle respectively and U is the electric potential of the trap and d is the radius of the trap. For motion in the radial direction the magnetic field will play a role. As a result the motion differs and there are two modes that can be found:

$$\omega_\pm = \frac{\omega_c}{2} \pm \sqrt{\frac{\omega_c^2}{4} - \frac{\omega_z^2}{2}}. \tag{2}$$

With

$$\omega_c = \frac{qB_0}{m} \tag{3}$$

being the cyclotron frequency and B_0 being the magnetic field. The frequencies ω_+ and ω_- being the so called modified cyclotron and magnetron frequencies respectively. Commonly $\omega_c > \omega_+ \gg \omega_z \gg \omega_-$, this being true as well in the ALPHA setup that will be discussed [9].

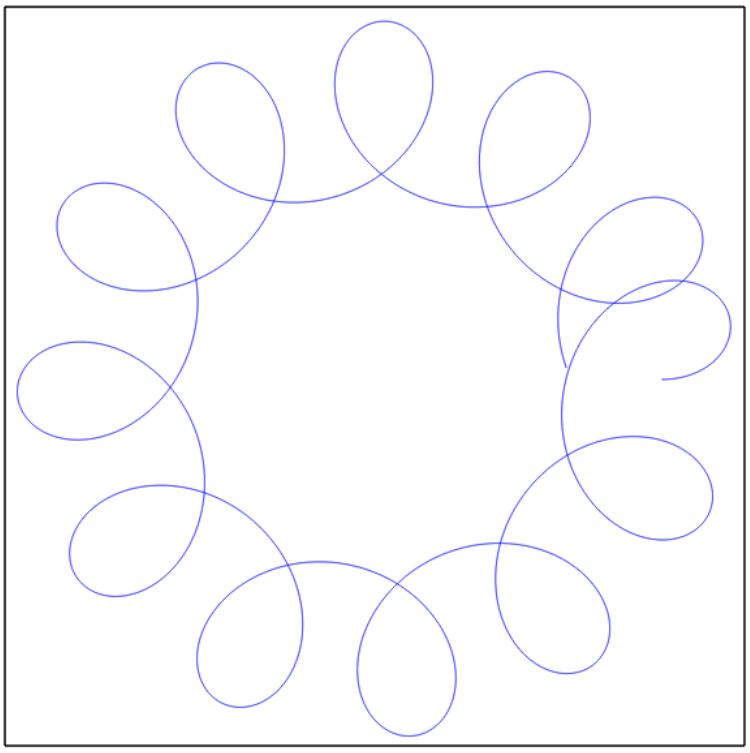

Figure 2: The radial motion of a particle in a Penning trap. The parameters have been so chosen as to exemplify the cyclotron and magnetron motion. In a trap $r_{\text{cyc}} \ll r_{\text{mag}}$ generally.

Geometrically these three modes of motion may be interpreted the faster cyclotron motion being superimposed on a slower magnetron drift motion. The total radial motion is shown in figure 1. In general the phases of the cyclotron motion do not line up with the magnetron motion which explains the jump that can be seen in the figure after one magnetron rotation. If one wants to make these phases line up, specific parameters have to be chosen [12]. The magnetron motion is also sometimes called the $\mathbf{E} \times \mathbf{B}$ drift motion since its direction is always in the $\mathbf{E} \times \mathbf{B}$ direction, independent of charge and mass. This speed and direction of this particular motion will as a result be equal for both positrons and antiprotons.

3.2 Antihydrogen Formation

To form antihydrogen an antiproton and positron must first be combined. In order to achieve this formation the positron must lose energy to be able to be bound to the antiproton. There are two main processes that are believed to be involved in this combination. The fist being radiative recombination. In this process the positron loses energy by photo emission;

$$e^+ + \overline{p} \rightarrow \overline{\mathrm{H}} + \gamma \tag{4}$$

While this process is relevant in many circumstances, for the temperature regime as seen in the particles captured at ALPHA (< 30 K) the actual probability of this radiative recombination occurring is very small when compared to the other processes involved [13]. The recombination rate (rate of antihydrogen production) has been found to be dominated by a $\propto \mathrm{T}^{-\frac{1}{2}}$ term by Müller *et al* [14]. While antihydrogen formed by this process could still produced in detectable quantities, the amount that would be trappable would be very small as explored by Robicheaux [15].

The other option, three-body recombination seems more promising. During three-body recombination the positron loses its energy via collision with another positron:

$$e^+ + e^+ + \overline{p} \rightarrow \overline{\mathrm{H}} + e^+. \tag{5}$$

The other positron will carry the excess energy away. This formation channel has a recombination rate that has a different temperature dependence when compared to the radiative recombination rate. The rate depends on $T^{-\frac{9}{2}}$ [16, 17] meaning that for lower temperatures the formation by three-body recombination should be dominating. This process then should explain the primary formation channel of antihydrogen for this temperature regime in a Penning trap. While the exact formation method of antihydrogen has eluded detection, measurements have been done by the ALPHA collaboration that imply field ionization of antihydrogen occurring [18]. This in turn implies that the antihydrogen detected is formed by three-body recombination. The reason behind this is that the antihydrogen is expected to be be weakly bound when formed by three-body recombination, whereas antihydrogen from two-body recombination is strongly bound [13]. The field of the ALPHA trap is not strong enough to field ionise strongly bound particles. So as a result the antihydrogen that was field ionised by the trapping field was very likely formed by three-body recombination.

3.2.1 Interactions After Formation

Since the antihydrogen has been formed in a dense positron plasma, interactions with positron are likely. After such a interaction the antihydrogen atom could be ionised, separating it back into its constituents.

$$e^+ + \overline{\mathrm{H}} \rightarrow \overline{p} + e^+ + e^+ \tag{6}$$

This implies that the positron in the formed antihydrogen must have sufficient binding energy to survive the plasma and be detectable. On the other hand, the anti-atoms may not necessarily be negatively effected by interactions with the plasma, the binding energy may also increase instead. This can occur when a positron "knocks" the atom into a lower exited state causing the binding energy to increase.

$$e^+ + \overline{\mathrm{H}}^{**} \rightarrow \overline{\mathrm{H}}^{*} + e^+ \tag{7}$$

Where $*$ represents some arbitrary exited state. Antihydrogen will generally be in an exited state when formed. This reaction has a favorable effect on the chance that an antihydrogen atom is detected, since it will decrease the probability that the otherwise weakly bound anti-atom will be ionised via reaction (6). Previous studies have found that the reactions (6), (5), and (7) are in equilibrium during the formation process [19].

4 Method

A number of aspects of the simulation of antihydrogen formation will be discussed here as well as the numerical methods employed. During formation a lot of physical effects are combined. In order to simulate these accurately considerations will have to be made on how to approach the problem. The part of the formation process that will be considered during the simulations will be focused on the "mixing" step where the antiprotons are combined with the positrons in the trap. Their combination will have to be simulated in the plasma that forms in the center of the trap. Since three-body recombination will be considered, the antiproton will be simulated inside of the positron. Here the positrons are numerous and interactions between them and the antiproton are more likely to result in antihydrogen forming through three-body recombination.

4.1 Numerically Solving the Equations of Motion

During combination the full equations of motion will have to be simulated in order to obtain an accurate result for a recombination event. The force on both the positrons and antiproton can be expressed with the Lorentz law

$$\mathbf{F} = q(\mathbf{E} + \mathbf{v} \times \mathbf{B}). \tag{8}$$

In case of $\mathbf{B} = B_0\hat{z}$ and by separating the equation into velocity and acceleration such that they can be solved with a finite difference method, the full equations of motion become

$$\begin{aligned} \frac{dv_x}{dt} &= \frac{q}{m}(E_x(\mathbf{r}) + v_y B_0) & \frac{dx}{dt} &= v_x \\ \frac{dv_y}{dt} &= \frac{q}{m}(E_y(\mathbf{r}) - v_x B_0) & \frac{dy}{dt} &= v_y \\ \frac{dv_z}{dt} &= \frac{q}{m}E_z(\mathbf{r}) & \frac{dz}{dt} &= v_z. \end{aligned}$$

These are valid for both positrons and antiprotons. With $E_i(\mathbf{r})$ being the sum of both the external field and the coulomb field created by other particles. To solve these six coupled differential equations a 4th-order Runge-Kutta numerical integration method will be used. The position and velocity at step $n+1$ is

$$\mathbf{r}_{n+1} = \mathbf{r}_n + \frac{h}{6}(\mathbf{k}_{r,1} + 2\mathbf{k}_{r,2} + 2\mathbf{k}_{r,3} + \mathbf{k}_{r,4}) \tag{9}$$

$$\mathbf{v}_{n+1} = \mathbf{v}_n + \frac{h}{6}(\mathbf{k}_{v,1} + 2\mathbf{k}_{v,2} + 2\mathbf{k}_{v,3} + \mathbf{k}_{v,4}) \tag{10}$$

where h is the time step and

$$\begin{aligned} \mathbf{k}_{v,1} &= \mathbf{a}(\mathbf{r}_n, \mathbf{v}_n) & \mathbf{k}_{r,1} &= \mathbf{v}_n \\ \mathbf{k}_{v,2} &= \mathbf{a}\left(\mathbf{r}_n + \frac{h}{2}\mathbf{k}_{r,1},\ \mathbf{v}_n + \frac{h}{2}\mathbf{k}_{v,1}\right) & \mathbf{k}_{r,2} &= \mathbf{v}_n + \frac{h}{2}\mathbf{k}_{v,1} \\ \mathbf{k}_{v,3} &= \mathbf{a}\left(\mathbf{r}_n + \frac{h}{2}\mathbf{k}_{r,2},\ \mathbf{v}_n + \frac{h}{2}\mathbf{k}_{v,2}\right) & \mathbf{k}_{r,3} &= \mathbf{v}_n + \frac{h}{2}\mathbf{k}_{v,2} \\ \mathbf{k}_{v,4} &= \mathbf{a}\left(\mathbf{r}_n + h\mathbf{k}_{r,3},\ \mathbf{v}_n + h\mathbf{k}_{v,3}\right) & \mathbf{k}_{r,4} &= \mathbf{v}_n + h\mathbf{k}_{v,3} \end{aligned}$$

Here $\mathbf{a}(\mathbf{r}, \mathbf{v})$ being the expression

$$\mathbf{a}(\mathbf{r}, \mathbf{v}) = \frac{d}{dt}\begin{bmatrix} v_x(\mathbf{r}, v_y) & v_y(\mathbf{r}, v_x) & v_z(\mathbf{r}) \end{bmatrix}^\top \tag{11}$$

and $\mathbf{v}$ and $\mathbf{r}$ being the regular velocity and position vectors.

4.1.1 Choice of Integrator

There are number of available approaches to integrate numerically, the Runge-Kutta seems like an appropriate choice for the problem. Its advantage lies in its accuracy above other methods like the Euler and leap frog approaches. While the other two methods require less integration steps as opposed to the RK method (one vs. four per time step respectively), the accuracy gained is well worth the extra time spend on integration. The solver requires high accuracy since the motions of the positrons around the antiproton can be quite fast as a positron reaches the minimal separation distance. At higher accelerations like this inaccuracies by the solver can cause large deviations from the real results.

Even with the additional steps the integration is not perfect. When examining the energy of certain systems solved by the RK4 method, it tends to diverge from the starting energy over time even though the conservation of energy should hold in said system. This is a clear indication that the solver is not symplectic. However, significant errors in the energy should not happen at short timescales if the integration step has been chosen to be sufficiently small. Other approaches are also available. Choosing a higher order ODE solver could result in energy conservation being maintained, with the trade off being even more integration steps and a more extensive implementation process. The other options is using a variable time step Runge-Kutta integrator that modifies its time step dynamically via the monitoring of one or more conserved quantities of the system. The main advantage of using this method is that it leads to an accurate solution while also decreasing

compute time by means of speeding up the simulation. This is achieved by the integrator increasing time step in areas of the simulation where less accuracy is required [20].

In view of the scope of the project a simple 4th order RK method will be implemented as shown in equations (9) and (10). The error it gives is acceptable for now; the timescales involved are sufficiently small. Additionally, it could be easily swapped out for another if the need were to arise. By selecting this integrator an appropriate time step will have to be chosen. This will be discussed in another section.

4.2 Feasibility of Full System Simulation

By having a method to solve the equations of motion of an arbitrary number of particles it would seem sensible to fully simulate all particles in the trap, in addition to the potential from the trap electrodes. This way a comprehensive simulation of the system could be explored. In the remainder of this section it will be shown how the computation of such a simulation will be difficult.

An essential part of the system is the process of mixing the antiprotons and positrons. When introduced to the positron plasma the antiprotons must first be able to enter this plasma through the z-axis. This would ordinarily not be possible since the positrons are trapped in a potential well, keeping them in but also keeping the oppositely charged antiprotons out. This is where the plasma screening comes in. The positron plasma will produce a self field and screen any external electric fields, meaning that inside of the plasma a particle would only experience this self field and not be influenced by an outer field. The characteristic length for this process is known as the Debye length

$$\lambda_D = \sqrt{\frac{\epsilon_0 k_B T}{n_e e^2}}, \tag{12}$$

where n_e is the number density of the positron plasma. For a positron plasma at 15 K with density $n_e = 10^{14}$ values typical in the trap, this length would be ≈ 26 μm. To observe screening, the dimensions of the plasma will have to be $\gg \lambda_D$. If the plasma radius was $10\lambda_D$, which would still be considered an edge case for plasma screening, the number of positrons in this plasma would be $\approx 1.5 \times 10^4$.

Suppose you were to introduce an antiproton to this plasma and study its interaction between the antiprotons and see if it forms antihydrogen. To fully simulate such a system all coulomb interactions between all positrons would have to be simulated. No shortcuts can be taken as the potential of all other positrons will influence the trajectory of a single positron. This means that the coulomb force will have to be computed for every particle on every other particle. The compute time that would be spend calculating the coulomb force would be $\propto N^2$, N being the number of particles that would have to be simulated.

As you may already see, such a computation might take a long time. Suppose it would cost only 10 ms to compute the trajectory of one particle (this is the lower end of compute time). For the small plasma of radius $10\lambda_D$ with $\approx 1.5 \times 10^4$ particles as discussed above the computation time could exceed 26 days. By using powerful super computers and by parallel computing of the coulomb force, a more reasonable time frame could be achieved. However, this would be out of the scope of this research. Furthermore, even if you were to to compute this plasma state fully, the actual positron plasma in the trap is at least 1 mm in the radial direction. With the small plasma you could only investigate the dynamics of antiprotons around the center of the trap. For antihydrogen formation at larger radii, more computational effort will have to be invested.

In conclusion, simulation of the full plasma is not reasonable within the scope of this research. If the plasma is taken to be to small, important properties of the system are lost, leading to potentially inaccurate results. If the system is large enough for the plasma to exhibit behaviour similar to that in the real trap, the simulation would take an unreasonable amount of time. Despite this, other options exist to simulate the recombination interactions.

4.3 Statistical Interaction Model

As discussed in section 4.2, full simulation of the system is not feasible. Instead a more traditional statistical interaction model will be used to simulate the three-body recombination formation process. The process is divided into two stages. Firstly the interaction probability between an antiproton and positron will be computed. A box of fixed size is drawn around the antiproton, it is always oriented in the direction of the velocity vector. This box will sweep out a volume $V = d^2|\mathbf{v}|\delta t$ in time δt, where d is the side length of the cube and $\mathbf{v}$ the velocity of the antiproton. The expected number of particles in this volume is then

$$N = d^2|\mathbf{v}|\delta t n_e \tag{13}$$

where n_e is the number density of the plasma the antiproton is traveling through. If δt is taken to be sufficiently small, the positrons in V can be seen as entering through the front face of the box. In this case the average number of particles that enter the box during time δt is N. To obtain an integer number of particles entering the box during δt, a random number is obtained from a Poisson distribution with $\mu = N$, where μ is the mean of the poison distribution.

The positrons will not be covering much distance in the radial direction, since they will be having fast cyclotron motion due to the magnetic field. With a radius of gyration in the order of 100 nm, it is unlikely that a positron will enter the box around the antiproton from this direction. The $\mathbf{E} \times \mathbf{B}$ motion of the positron has a larger radius and will thus cover more distance. Despite this it is still highly unlikely that positrons will enter the box this way, as $v_{\mathbf{E}\times\mathbf{B}} \ll v_{\overline{p}}$ in general.

While constrained in the radial direction by the magnetic field, positrons may still enter from the z-axis since the self field of the plasma does not act axially and the magnetic field does not affect them when traveling in this direction. In this case the number interactions in δt becomes

$$N_z = \sigma \langle v_z \rangle \delta t n_e, \tag{14}$$

where $\langle v_z \rangle$ is the expectation value of the velocity of positrons in the z direction and σ is the interaction surface of the box around the antiproton.

This interaction surface is the part of the box that is oriented towards the z-axis in the frame of the plasma. This is given by

$$\sigma = d^2(\hat{e_1} \cdot \hat{z}) + d^2\sqrt{1 - (\hat{e_1} \cdot \hat{z})^2} \tag{15}$$

with $\hat{e_1} \equiv \frac{\mathbf{v}}{|\mathbf{v}|}$ and $\hat{e_2}$ being the orthogonal basis vector constructed from $\hat{e_1}$ and $\hat{z}$ by the Gram-Smith procedure. Since $\hat{e_1}$ and $\hat{e_2}$ are in same plane as $\hat{z}$, and $\hat{e_3}$ also an orthogonal basis vector, $\hat{e_3} \cdot \hat{z} = 0$. Just like with equation (13) the actual number of positrons in a given δt will be obtained via a Poisson distribution.

4.4 Simulation of Antihydrogen Formation

After knowing the probability that a positron will enter a box around the antiproton, the positrons will be introduced to the box accordingly. After a time frame δt a number of positrons will hence be found on the boundary of the cube around the antiproton (0, 1, 2...). After being introduced, the equations of motion will be solved for all particles inside the box as discussed in section 4.1. While the equations of motion are being solved new positrons may also be introduced to the box. If the particles leave the box they will be removed from the simulation. This was done to save computational time.

When two simulated positrons have a coulomb collision near the antiproton, there will be a chance that antihydrogen is formed. Antihydrogen is in this case defined as one positron being in the box with negative total energy in the antiproton reverence frame. The energy of a single positron near an antiproton is given by

$$V = \frac{1}{2}m_{\overline{p}}|\mathbf{v}_{\overline{p}}|^2 + \frac{1}{2}m_e|\mathbf{v}_e|^2 - \frac{e^2}{4\pi\epsilon_0 r}, \tag{16}$$

with r being the separation between the positron and antiproton. In figure 3 the process of formation is shown diagrammatically. In the figure the final negative energy is defined as a positive binding energy E_B. This binding energy is the minimal energy required for ionisation.

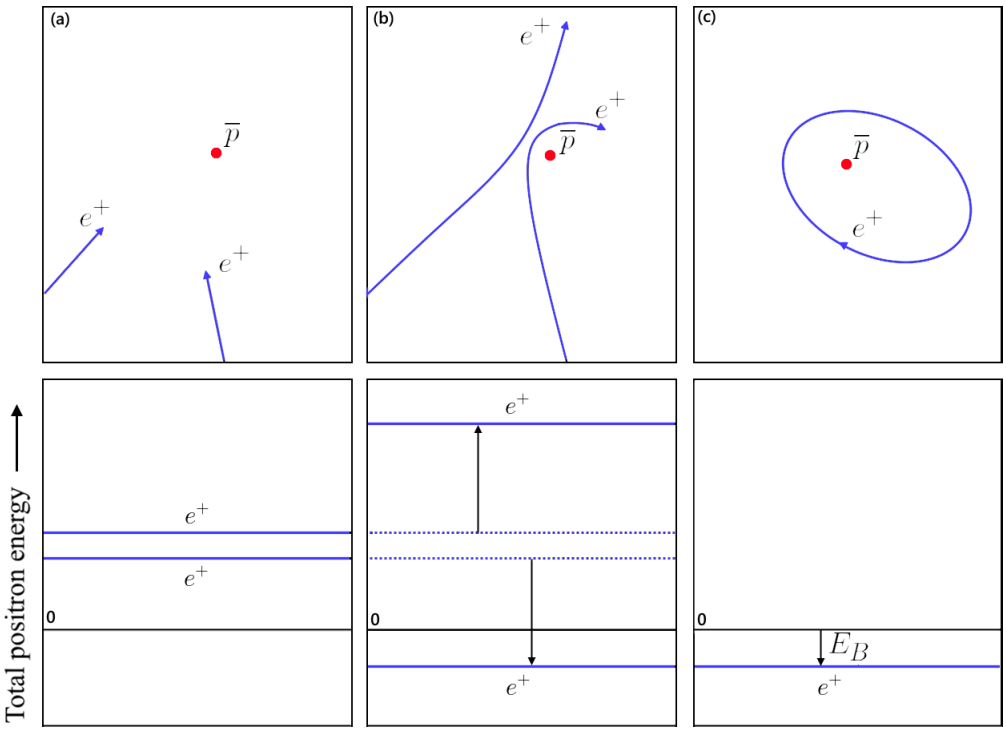

Figure 3: A diagram of the a classical 3 body recombination interaction. The top images show the stages of the interaction. The bottom graphs show the corresponding total positron energy (kinetic and electrostatic potential) of each of the positrons. **(a)** The positrons both move freely through space: both of their energies are higher then zero. **(b)** The positrons collide in the presence of the antiproton potential. In this case one of the positrons loses enough energy that its total is now below zero. The other positron gains the same amount of energy. **(c)** The positron is bound to the antiproton since its energy is lower then zero. This system is now considered antihydrogen. The binding energy of the positron is E_B in the antiproton frame.

While figure 3 gives an overview of the dynamics that occur during the collision and subsequent formation, it only shows the traces of the involved particles without any magnetic field being present. This is done to clarify the situation and provide an idea of the general process of three-body recombination. In the case of antihydrogen formation at ALPHA the situation changes. A strong magnetic field is now applying a force on particles. This will change the trajectory of the positron around the antiproton, it will no longer be an ellipse, as shown in figure 4. Not only will the trajectories change meaningfully, the rate at which recombination occurs will also be modified by the magnetic field [17] [21]. In this case the rate of recombination will be lowered by the presence of the magnetic field

4.5 Selection of the Time Step

A number of parameters will need to be selected, like the time step and the side of the interaction box. For the time step required it will be necessary to look at sources possible sources of error. During the the three-body recombination procedure Coulomb collisions are important. Hence they will need to be simulated with a certain level of accuracy. A procedure to achieve this has been outlined by Sillitoe and Hilico [22]. Briefly, to do this a minimum time step required can be estimated by taking the energy at the point of closest approach b and equating that to the kinetic

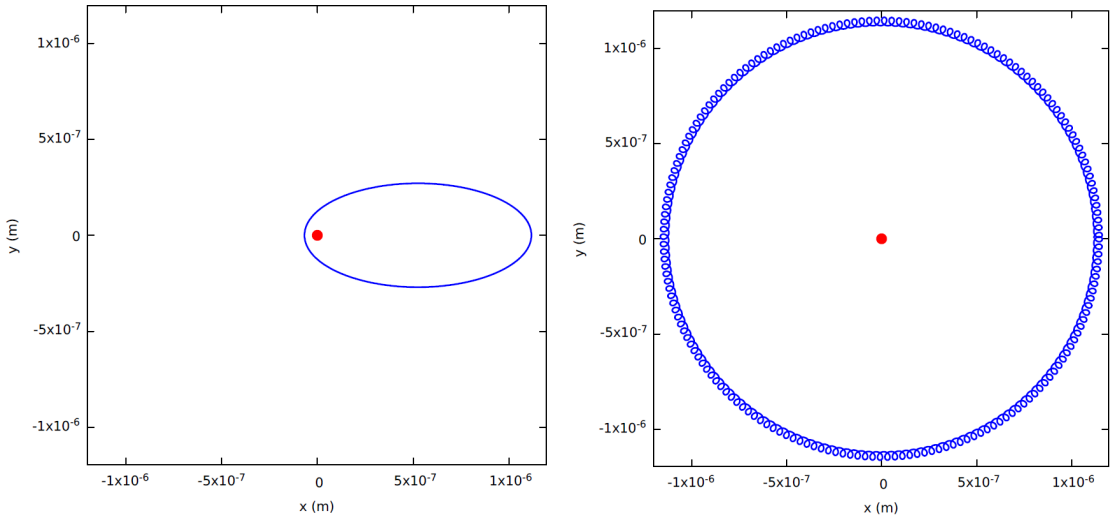

(a) Atom with $B = 0$.

(b) Atom with $B = 1$ T.

Figure 4: Two classical antihydrogen atoms, both with an identical binding energy of 14 K. The red dot represents the antiproton, the blue line is the trace of the positron. (a) has no magnetic field. (b) has a 1 T magnetic field in the z direction. No external electric field is present.

energy: $\mathrm{E_{coll}} = \frac{e^2}{4\pi\epsilon_0 b} = \frac{1}{2}mv_{max}^2$. For a time step δt the condition $v\delta t \ll b$ must hold. Then, since b is not always known an estimate can be made based on temperature. The requirement for δt then becomes

$$\delta t \ll \frac{e^2}{4\pi\epsilon_0}\frac{\sqrt{m}}{\sqrt{2}(k_B T)^{3/2}}. \tag{17}$$

For 15 K this results in a requirement that $\delta t \ll 10^{-12}$ s. This criterion is not strict but it would still be recommended to stay underneath the value that results from equation (17). To achieve this a value of 10^{-13} s is selected. This is in case there are multiple particles in the box and collisions will need to be taken into account. In case there are no particles in the box with the exception of the antiproton, a time step value of 10^{-9} s is chosen instead. This is done to decrease the time spend on simulating the motion of the antiproton when no positrons are near it.

4.6 Interaction Box Size

The size of the interaction box plays an important role in eventual formation of antihydrogen. If the box is chosen to be too small it may occur that a positron will instantly form antihydrogen when it enters the box, with no three-body recombination being involved. Physically the positron would have had time to accelerate towards the positron before it would enter the box, causing it to always have positive potential energy (assuming no third body was present). However, in the simulation, the particle will be introduced on one of the faces of the box discontinuously causing it to have a negative potential energy that is not connected to its kinetic energy. Which as said before could cause formation to occur even though no three-body recombination has happened. To minimise this probability a box size will have to be chosen such that the potential energy that corresponds to its size is much larger then the size of an antihydrogen atom at the typical kinetic energies of the positrons. If a positron is introduced to the side of a box that follows these criteria the particle will be very unlikely to be bound to the positron as it will almost always have a kinetic energy higher then its electrostatic potential energy. To find the length that is associated with temperature, the size of a formed antihydrogen atom will need to be found first. The classical radius of an antihydrogen atom is

$$r = \frac{e^2}{4\pi\epsilon_0 k_B T}, \tag{18}$$

where T is the energy of the positron around the antiproton. At a temperature of $T = 15$ K, this would correspond to a radius of $r_{\max} = 1.1$ μm. If the box would be smaller than this radius, a positron with kinetic energy equal to 15 K would be bound as soon as it enters the box, assuming that the antiproton has no kinetic energy. When the positrons are at an average temperature of 15 K this may occur often.

To reduce these false formation events a larger box has to be selected. However in case the box is selected to be too large, many particles will enter it, causing a slowdown of the simulation. After testing the performance of a number of sizes a trade-off was achieved where the side length of the box was chosen to be $20r_{\max}$.

4.7 Thermal Conditions

In the simulation of the system thermal conditions will have to be taken into account. This will be implemented with the assumption that the system will be in thermal equilibrium. It is taken that this is a reasonable assumption for the positrons as they are moving around confined in the trap in a fixed volume during the mixing stage. Furthermore, the positrons will cool due to the cyclotron radiation, meaning any thermal fluctuations will be resolved and the system will be brought back to an equilibrium. The assumption that the antiproton will also be in equilibrium is more tenuous. Antiprotons that are brought into the positron plasma will not necessarily have the same thermal equilibrium, as a result, the antiprotons will have a differing mean velocity. Nevertheless, the antiprotons are still expected to reach thermal equilibrium with the plasma they are inserted into quickly (in the order of μs, provided the initial temperatures do not differ too much). This occurs due to a number of effects like slowing in the plasma due to plasma waves [23] and the antiproton slowing down due to Coulomb interactions with the colder positrons [24]. It is for this reason that the assumption is maintained that the antiproton will be in thermal equilibrium with the positrons, since this will reflect the situation as seen shorty after the insertion of the antiprotons.

In practice, when staring the simulation or when a new positron enters the box, all particles will be initialised according to a Maxwell-Boltzmann distribution with the same temperature. This will be done by initializing the involved particles with x, y, and z velocities according to to a normal distribution. Each of these having a standard deviation $\sqrt{k_B T/m}$, and a mean of zero.

4.8 Plasma State in the Simulation

While the state of the plasma can be quite complicated and depend on many factors, simplifications can be made that make it easier to express in the simulation. The elements of the plasma that are of interest are the density and the self-field that dominates inside the plasma. The density of the plasma is used in equations (13) and (14). To solve the equations of motion of particles inside the plasma the electric field must be known. By solving the Laplace equations an electric field can be obtained inside the plasma, in this case only the radial field remains: [23]

$$\mathbf{E}_r = \frac{n_e e r}{2\epsilon_0}\hat{\rho}. \tag{19}$$

Where r is the distance to the center of the plasma and $\hat{\rho}$ is the radial direction away from the center. The equation also depends on n_e uniformly. During the simulation it is assumed that n_e remains the same over time. In addition n_e will not vary in space. The plasma will fill all of space for the simulations, but can always be limited in size later on. Note how the radial electric field is similar to the radial Penning trap field. This field also points outward and increases with distance to the center of the trap. As a result the motion of all particles in the plasma will be similar to that in a Penning trap, with the exclusion of the axial motion which is not present in the plasma. Instead the particles will be free to move in the axial direction since there is no electric field in this direction.

5 Results & Discussion

For the following results an antiproton has been released at a specified radial distance from the center. Each time the particle was released it would be at a thermal velocity with the same temperature distribution as the positron plasma. The temperature used was 15 K unless specified otherwise.

5.1 Binding Energies of Newly Formed Antihydrogen

The antiprotons are released one by one and allowed to drift for 100 μs, or until they form an antihydrogen atom. They are released at $r = 0$, the center of the plasma. The binding energies of these antihydrogen atoms are recorded. Since the simulation is stopped the moment an antihydrogen is formed the values of the binding energies will be those at the moment of formation. The distribution of the binding energies of 829 antihydrogen atoms can be seen in figure 5.

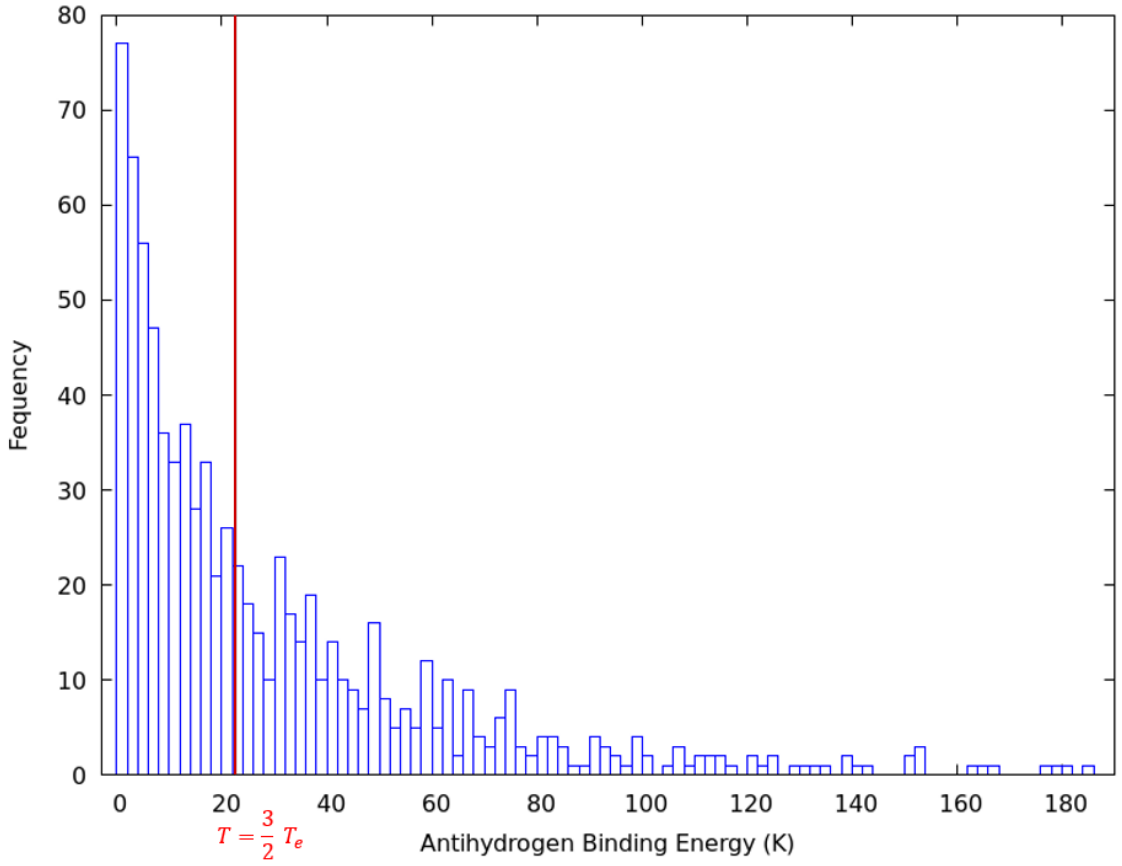

Figure 5: The distribution of binding energies in K of a newly formed antihydrogen. The number of antihydrogen instances recorded was 829. The red line indicates the mean energy of the positron plasma with temperature $T_e = 15$ K.

The distribution of the antihydrogen shown is formed in a plasma with a number density of 10^{13} m^{-3} and a temperature of 15 K. Note the long tail on the exponential distribution. Figure 5 has been truncated to focus on the lower temperature binding energies. Events continue to get sparser as the binding energies increase, with a few outliers having binding energies over 1000 K. Note that some higher binding energies may not be physical. A high binding energy indicates that a positron has a small separation distance with a antiproton, corresponding to a high velocity. Since the numerical solver uses a fixed time step, the error of computation will increase as the

positron gets closer to the antiproton. The distributions of the binding energy should not depend on the number density of the positrons, only the rate of interaction should (like in figure 8). This is shown in figure 6. Note that the sampling size was lower when compared to figure 5, leading to a greater statistical error.

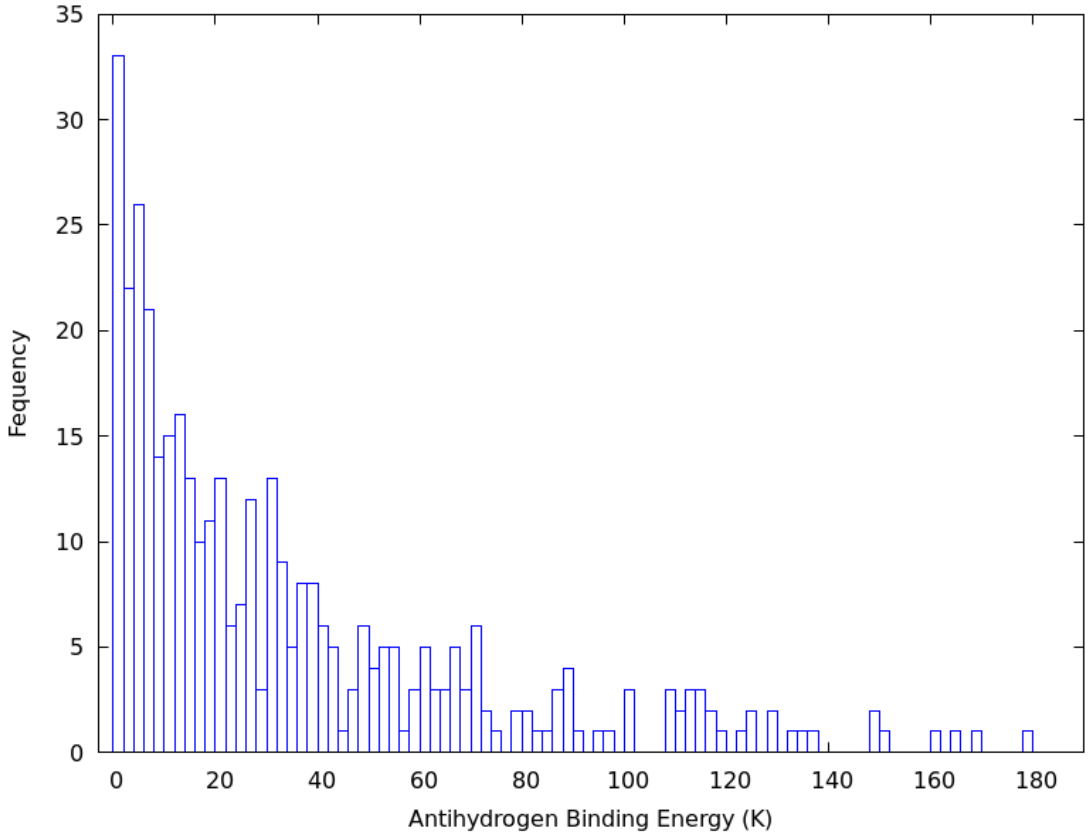

Figure 6: Distribution of antihydrogen binding created from the same circumstances as 5 but with a positron plasma that has $n_e = 10^{14}$ m^{-3}. The sampling size was 385 antihydrogen events.

On both of these figures it can be seen how the binding energies follow an exponential distribution. The binding energies that seem to be most common are those in the order of the temperature of the surrounding positron plasma. This is in accordance with earlier predictions that have also suggested the dominance of thermal binding energies as a result of three-body recombination [15]. To put the binding energies into perspective, it should be mentioned that the energies that are associated with this three-body recombination are low. For comparison, the energy of a ground state antihydrogen atom would be 1.58 $\times 10^5$ K. This means that the antihydrogen formed due to three-body recombination is in a highly exited state, as mentioned in section 3.2. These very low binding energies would also result in a much higher probability of re-ionization immediately after being formed. Since formation would occur inside the dense positron plasma, the newly formed antihydrogen would be very likely to interact with another positron. These positrons are likely to re-ionise the formed antihydrogen since the binding energies will be similar to the energy of the surrounding plasma. The mean energy of the plasma is shown as a red line in figure 5 ($\frac{3}{2}\,T$, assuming the plasma is Maxwell-Boltzmann distributed). The line serves as a reference when comparing the binding energy to the thermal energy. All antihydrogen that formed to the left of this line is more likely to get ionized via positron collision. The "deeper" bound states are less likely to get ionized. From the figure it can be seen that the energy of the antihydrogen is generally insufficient to prevent it from being ionized in most circumstances; most antihydrogen will be ionized immediately after its formation.

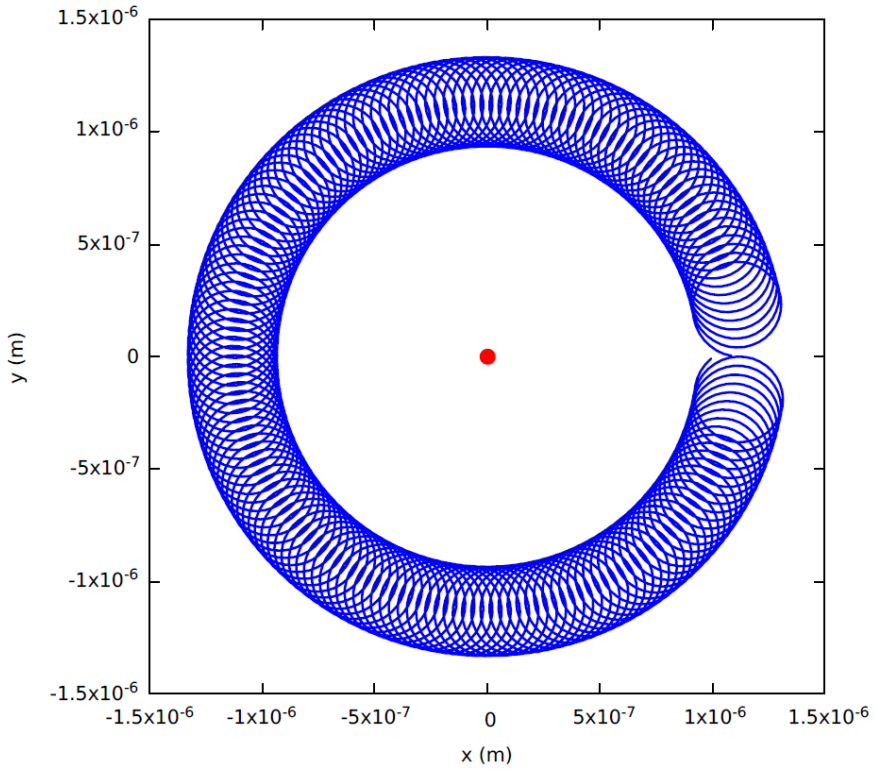

Figure 7: Meta-stable classical antihydrogen, where the positron has positive energy, yet, still remains near the antiproton. No external electric field is present. With external magnetic field of 1 T in the z direction.

Not only the surrounding positrons play a role in re-ionisation. The electric field may also cause the destruction of the anti-atom. If the positron is lightly bound to the antiproton, it may occur that the positron will be ripped away by a stronger electric field. The always present external magnetic field may prevent this from happening for lower electric field strengths, but at a certain point the strength of the field will be too high and ionization will occur. As mentioned in section 4.8, inside the plasma the electric field will increase radially. So it could be that the antihydrogen is more likely to get ionized the further from the center of the plasma. Although it would not be obvious at what field potential the antihydrogen would re-ionize due to the presence of the magnetic field.

5.1.1 Meta-Stable States

The magnetic field may also cause other unexpected effects to occur. When a strong magnetic field is present, the result may be a meta-stable state of antihydrogen. Antihydrogen is defined as a positron having a negative total energy with respect to an antiproton. This, however, is not the only stable state that is possible. When a magnetic field is present, the positron may still remain near the antihydrogen even if its total energy is positive. These states are unaccounted for in the binding energy distributions since the criterion for formation of antihydrogen was a negative total energy. The “antihydrogen” in these states could be detected, although they will also be more susceptible to ionization by both electric field and other particles, since it will be bound even weaker. As a result the probability that the antihydrogen survives long enough will be lower. In figure 7, a classical simulation of such a meta-stable state can be seen.

5.2 Correspondence With Quantum Mechanics

As mentioned previously, the binding energies of the antihydrogen suggest a highly exited state. This state may be expressed as the principal quantum number. In order to give an idea of the quantum numbers involved a number of assumptions are made to go from a classical binding energy to the principal quantum number. Th binding energy will be equated to the principal quantum number,

$$n = \sqrt{\frac{13.6[\text{eV}]}{E_B}}, \tag{20}$$

under the assumption that the angular momentum quantum number is zero. If E_B would be 15 K, $n \approx 103$. For these binding energies the principal quantum number is high enough that a classical simulation is justified for the phenomenon of three-body recombination. Even though this may the case the system is still not in the classical limit $n \to \infty$, resulting in a difference between physical values of the binding energy and those obtained in the simulation. Despite this, a classical simulation would still be the most feasible option, since a quantum mechanical calculation would be much more computationally demanding especially for the amount of events being recorded. Alternatives like this do exist however and could potentially be employed to gain insight in certain aspects of antihydrogen formation. Aspects of three-body recombination of hydrogen have been investigated attempting to approximate quantum mechanical details of the system [17].

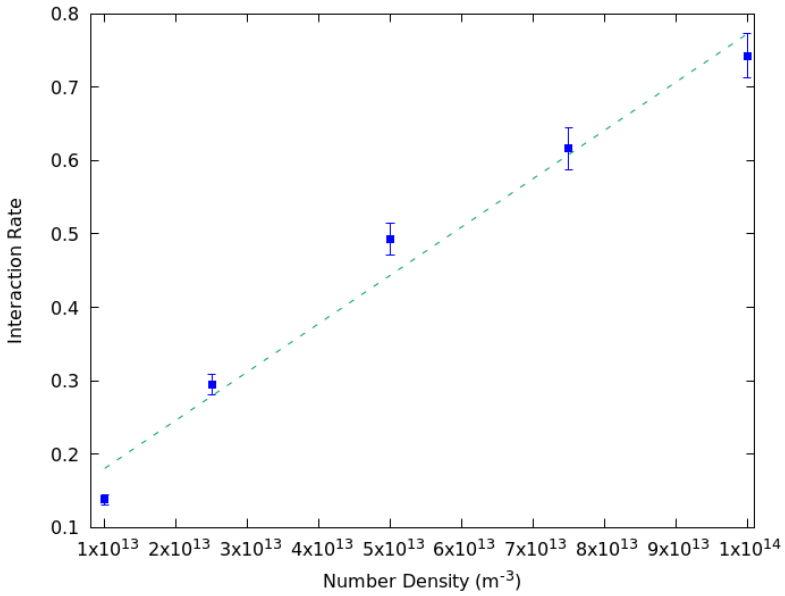

Figure 8: The interaction rate of antihydrogen formation for a range of number densities of the positron plasma. The fit shows that the rate is approximately proportional to n_e.

5.3 Three-Body Interaction Rate

By taking the number of antiprotons released against the number that formed antihydrogen, an interaction rate can be obtained. The antiprotons were simulated for a time 100 μs or until the antiproton formed antihydrogen. As formulated by theory the interaction rate should be linearly proportional to the number density of the positrons. The interaction rate is therefore simulated for various values of n_e that are within the range of the values as they occur at ALPHA. The results can be seen in figure 8

The slope in this graph should be the three-body recombination coefficient. For both no magnetic field and $B \to \infty$ field strength the values for this coefficient have been obtained theoretically

[17, 25]. In other simulation work this constant was also computed for a finite non-zero magnetic field [21]. Although the rate approximately proportional to n_e, the fit that is introduced is too low confidence to extract a three body recombination rate from it. More work will be needed to obtain this interaction coefficient. However this simulation method should eventually be ably to obtain a reasonable estimate of the recombination rate.

5.4 False Events

One of the reasons why the confidence in the number of interactions is still low is interference due to very low binding energy false positives. These are "antihydrogen" events originating from a positron entering the interaction box and discontinuously gaining an electrostatic potential as discussed in section 4.6. While the selection of side of the box should reduce the probability of this type of interaction occurring, it is nonetheless still possible.

To show this effect, the interaction rate for lower temperatures is shown without changing the box size. In figure 9 this rate is plotted as the temperature decreases. As was discussed in section 3.2, the rate of three-body formation should be proportional to $T^{-9/2}$, instead the graph shows a proportionality of T^{-1}. The reason behind this is the previously mentioned instant formation of the antihydrogen as positrons enter the box. Since the radius at which this formation happens is $\propto T^{-1}$ per equation (4.6), it makes sense that the rate of formation would also have this proportionality.

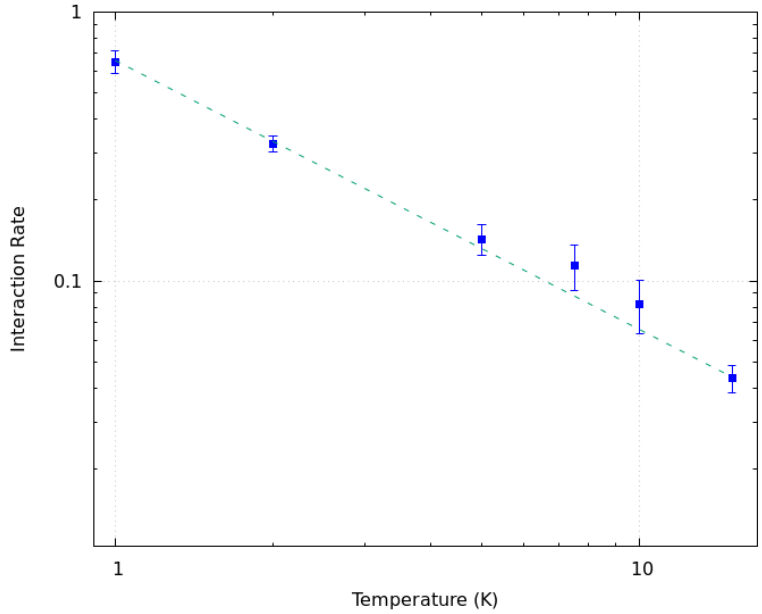

Figure 9: The interaction rate vs the temperature of the positron plasma. Plotted in a double log scale. This is the interaction rate for an interaction box that has been set at $r_{\max}$ for 15 K and has not been increased in size as T decreases (see section 4.6). The dotted line is $\propto T^{-1}$.

So, how would we obtain a correct method for rejecting these events? If we make the box larger there are two problems. Firstly, the criterion for formation would be harder to determine. As the box increases in size, it is less likely for there to be only one positron in the box. Another formation criterion will need to be implemented. Secondly, the number of particles in the box will start increasing quickly as $T \to 0$ and the box size will tend to infinity, slowing down the simulation considerably, as discussed in 4.2. Another method will need to be found and implemented to reject false events from the formation rate. While these false events interfere with the ability to simulate formation rates, the effect is limited on the binding energy distribution. For a distribution with a box that corresponds to the temperature of the surrounding positrons, like figures 5 and 6, the effect can only appear for binding energies < 1.5 K. This is the temperature associated with the length of the side of the box.

6 Conclusion

A model has been outlined that simulates the the formation of antihydrogen, through three-body recombination, under circumstances similar to that in an antihydrogen formation experiment like ALPHA. This was achieved through a classical, numerical solution of the equations of motion of the positrons and antiprotons in an external magnetic and electric field. Since full simulation of the system was found to be unfeasible, a statistical approach was selected instead. This approach would only compute the full equations of motion of positrons around the antiprotons in a box of limited size. After interactions were simulated, antihydrogen formation events would be determined based on the energy of a single positron near an antiproton, in the antiproton frame. Most of the antihydrogen formation events that were found, had an associated binding energy that was in the order of mean energy of the formation environment, with deeper bound stated being less common. This indicates that most antihydrogen formation that occurs through three-body recombination, is lightly bound, and will not survive long under the circumstances of its formation, ionizing through either field-ionization or though collisions with other positrons of similar energies.

While this simulation method managed to successfully simulate formation of antihydrogen through classical three-body interactions and record its binding energy, more work will be required to simulate other aspects of this process accurately. The current method, for example, only simulated up to the moment of formation and does not take into account anything that happens afterwards. Simulating the binding energy is an important first step in eventually determining whether an antihydrogen atom will survive long enough to be detectable and measurable, but a more comprehensive model will be needed to simulate the full lifetime of the newly formed antihydrogen. Other aspects, like the false formation events, also pose an issue for determining aspects like the formation rate, and will need to be resolved to gain insight into the number of formed antihydrogen atoms, for a given number of antiprotons.

Despite this, the model offers a starting point for simulations of the formation of antihydrogen. The classical simulation offers an approachable method, that is not as computationally intensive as a quantum mechanical simulation would be, while still capturing the process with acceptable accuracy due to the high principal quantum number of the formed antihydrogen. For these reasons this relatively simple model can be used as a stepping stone to even better understand the complex dynamics of antihydrogen formation.

Acknowledgements

Special thanks to Steve Jones, whose guidance, feedback and insightful discussions greatly helped me with this project. I would also like to extend my thanks to the rest of the DiCE group: Nikos, Tom and Sam, who were amazing colleagues that helped me along the way.

References

[1] Carl D Anderson. "The positive electron". In: *Physical Review* 43.6 (1933), p. 491.

[2] Paul Adrien Maurice Dirac. "The quantum theory of the electron". In: *Proceedings of the Royal Society of London. Series A, Containing Papers of a Mathematical and Physical Character* 117.778 (1928), pp. 610–624.

[3] M. Ahmadi et al. "Observation of the 1S-2S transition in trapped antihydrogen". In: *Nature* 541.7638 (2017), pp. 506–512. ISSN: 14764687. DOI: 10.1038/nature21040.

[4] F. Robicheaux. "Simulations of antihydrogen formation". In: *Physical Review A - Atomic, Molecular, and Optical Physics* 70.2 (2004), pp. 1–5. ISSN: 10502947. DOI: 10.1103/PhysRevA.70.022510.

[5] S. Jonsell and M. Charlton. "On the formation of trappable antihydrogen". In: *New Journal of Physics* 20.4 (2018). ISSN: 13672630. DOI: 10.1088/1367-2630/aabc71.

[6] C. Amole et al. "The ALPHA antihydrogen trapping apparatus". In: *Nuclear Instruments and Methods in Physics Research Section A: Accelerators, Spectrometers, Detectors and Associated Equipment* 735 (Jan. 2014), pp. 319–340. ISSN: 0168-9002. DOI: 10.1016/J.NIMA.2013.09.043.

[7] C. J. Baker et al. "Sympathetic cooling of positrons to cryogenic temperatures for antihydrogen production". In: *Nature Communications* 12.1 (2021). ISSN: 20411723. DOI: 10.1038/s41467-021-26086-1.

[8] W. A. Bertsche. "Prospects for comparison of matter and antimatter gravitation with ALPHA-g". In: *Philosophical Transactions of the Royal Society A: Mathematical, Physical and Engineering Sciences* 376.2116 (2018), p. 20170265. DOI: 10.1098/rsta.2017.0265. eprint: https://royalsocietypublishing.org/doi/pdf/10.1098/rsta.2017.0265. URL: https://royalsocietypublishing.org/doi/abs/10.1098/rsta.2017.0265.

[9] Mike Charlton and Dirk Peter van der Werf. "Advances in antihydrogen physics". In: *Science Progress* 98.1 (2015), pp. 34–62. ISSN: 20477163. DOI: 10.3184/003685015X14234978376369.

[10] M. Ahmadi et al. "Antihydrogen accumulation for fundamental symmetry tests". In: *Nature Communications* 8.1 (2017), pp. 1–6. ISSN: 20411723. DOI: 10.1038/s41467-017-00760-9.

[11] C. J. Baker et al. "Laser cooling of antihydrogen atoms". In: *Nature* 592.7852 (2021), pp. 35–42. ISSN: 14764687. DOI: 10.1038/s41586-021-03289-6.

[12] Manuel Vogel. *Particle Confinement in Penning Traps*. Vol. 100. 2018. ISBN: 978-3-319-76264-7. URL: http://www.springer.com/series/411.

[13] Michael H. Holzscheiter, Michael Charlton, and Michael Martin Nieto. "The route to ultra-low energy antihydrogen". In: *Physics Reports* 402.1-2 (2004), pp. 1–101. ISSN: 03701573. DOI: 10.1016/j.physrep.2004.08.002.

[14] Alfred Müller and Andreas Wolf. "Production of antihydrogen by recombination of p with e+: What can we learn from electron-ion collision studies?" In: *Hyperfine Interactions* 109.1-4 (1997), pp. 233–267. ISSN: 03043843.

[15] F. Robicheaux. "Atomic processes in antihydrogen experiments: A theoretical and computational perspective". In: *Journal of Physics B: Atomic, Molecular and Optical Physics* 41.19 (2008). ISSN: 09534075. DOI: 10.1088/0953-4075/41/19/192001.

[16] G. Gabrielse et al. "Possible antihydrogen production using trapped plasmas". In: *Hyperfine Interactions* 44.1-4 (1989), pp. 287–293. ISSN: 03043843. DOI: 10.1007/BF02398677.

[17] Michael E. Glinsky and Thomas M. O'Neil. "Guiding center atoms: Three-body recombination in a strongly magnetized plasma". In: *Physics of Fluids B* 3.5 (1991), pp. 1279–1293. ISSN: 08998221. DOI: 10.1063/1.859820.

[18] G. B. Andresen et al. "Trapped antihydrogen". In: *Nature* 468.7324 (2010), pp. 673–676. ISSN: 00280836. DOI: 10.1038/nature09610.

[19] S. Jonsell, M. Charlton, and D. P.Van Der Werf. "The role of antihydrogen formation in the radial transport of antiprotons in positron plasmas". In: *Journal of Physics B: Atomic, Molecular and Optical Physics* 49.13 (2016). ISSN: 13616455. DOI: 10.1088/0953-4075/49/13/134004.

[20] William H Press et al. *Numerical recipes 3rd edition: The art of scientific computing*. Cambridge university press, 2007. Chap. 9.

[21] F. Robicheaux and James D. Hanson. "Three-body recombination for protons moving in a strong magnetic field". In: *Physical Review A - Atomic, Molecular, and Optical Physics* 69.1 (2004), p. 4. ISSN: 10941622. DOI: 10.1103/PhysRevA.69.010701.

[22] Richard C Thompson, Niels Madsen, and Martina Knoop. *Trapped charged particles: a graduate textbook with problems and solutions*. Vol. 1. World Scientific, 2016. Chap. 8, pp. 161–177.

[23] Daniel H.E. Dubin and T. M. O'Neil. "Trapped nonneutral plasmas, liquids, and crystals (the thermal equilibrium states)". In: *Reviews of Modern Physics* 71.1 (1999), pp. 87–172. ISSN: 00346861. DOI: 10.1103/revmodphys.71.87.

[24] G Gabrielse et al. "First positron cooling of antiprotons". In: *Physics Letters B* 507.1 (2001), pp. 1–6. ISSN: 0370-2693. DOI: https://doi.org/10.1016/S0370-2693(01)00450-6. URL: https://www.sciencedirect.com/science/article/pii/S0370269301004506.

[25] Peter Mansbach and James Keck. "Monte Carlo Trajectory Calculations of Atomic Excitation and Ionization by Thermal Electrons". In: *Phys. Rev.* 181 (1 May 1969), pp. 275–289. DOI: 10.1103/PhysRev.181.275. URL: https://link.aps.org/doi/10.1103/PhysRev.181.275.